Supplementary material for article

The Jurassic magmatism of the Demerara Plateau (offshore French Guiana) as a remnant of the Sierra Leone hotspot during the Atlantic rifting

Christophe Basile[1] (corresponding author), Igor Girault[1*], Jean-Louis Paquette[2], Arnaud Agranier[3], Lies Loncke[4], Arnauld Heuret[5], Ewald Poetisi[6]

[1] Univ. Grenoble Alpes, Univ. Savoie Mont Blanc, CNRS, IRD, IFSTTAR, ISTerre, 38000 Grenoble, France. christophe.basile@univ-grenoble-alpes.fr
[2] Université Clermont Auvergne, CNRS, IRD, OPGC, Laboratoire Magmas et Volcans, F-63000 10 Clermont-Ferrand, France. J.L.Paquette@opgc.univ-bpclermont.fr
[3]Laboratoire Géosciences Océan (UMR CNRS 6538), Université de Bretagne Occidentale & Institut Universitaire Européen de la Mer, Place Nicolas Copernic, 29280 Plouzané, France. arnaud.agranier@univ-brest.fr
[4] Université de Perpignan, CEFREM – UMR 5110, 66860 Perpignan France. lies.loncke@univ-perp.fr
[5] Université de Guyane, Géosciences Montpellier 97300 Cayenne, France. arnauld.heuret@univ-guyane.fr
[6] Anton de Kom University of Suriname, Paramaribo, Suriname, SA. ewald.poetisi@uvs.edu
[*] Present address IDEES (UMR 6266 CNRS), Université de Rouen, France. igor.girault@univ-rouen.fr

Supplementary material includes the geochemical analysis (table 1), and four figures related to geochemical analysis (S4), their interpretation (S1 and S2), and past kinematic reconstruction (S3).

Table S1. Chemical analysis of magmatic DRADEM samples

	Samples												standards			
	DRA-C1-1	DRA-C1-2	DRA-C2-1	DRA-E1-8c-12	DRA-E1-9b	DRA-E1-9d	DRA-E1-1C	DRA-E1-1D	DRA-E1-2	DRA-E1-4	DRA-E1-5	DRA-E1-8b-3	BHVO2	BHVO2 (duplicate)	BIR1	BCR2
Petrology	rhyolite	rhyolite	basalt	interm.	interm.	interm.	interm.	interm.	interm.	interm.	interm.	interm.				
ICPOES (wt)																
SiO2	73.4	72.3	47.2	49.2	45.2	47.7	47.6	45.6	47.7	48.1	45.3	49.1				
TiO2	0.5	0.5	3.0	3.4	2.7	3.4	3.9	3.5	3.2	3.9	3.6	4.1				
Al2O3	11.5	11.7	14.2	15.6	16.1	15.6	15.5	16.9	18.4	18.5	17.4	15.7				
Fe2O3	2.5	2.7	13.3	13.7	12.9	12.9	13.9	9.6	9.1	9.6	8.8	10.7				
MnO	0.0	0.0	0.2	0.2	0.1	0.1	0.2	0.0	0.6	0.1	0.1	0.3				
MgO	0.2	0.3	5.3	2.7	4.0	3.5	3.8	3.0	3.8	3.0	3.0	2.9				
CaO	1.3	1.1	8.9	2.5	4.4	2.1	1.4	6.9	4.0	4.9	7.4	3.5				
Na2O	3.1	3.2	3.1	5.5	3.8	3.9	5.0	2.6	3.0	3.0	2.8	5.0				
K2O	4.5	4.6	1.0	2.1	2.3	3.7	1.3	3.4	3.2	2.6	3.1	2.0				
P2O5	0.1	0.1	0.4	0.4	1.5	0.5	0.5	0.4	0.4	0.4	0.4	0.5				
LOI	0.3	0.3	2.1	3.2	6.0	5.2	5.8	7.1	5.1	4.8	7.1	4.7				
Total	97.5	96.7	98.8	98.6	99.0	98.6	99.0	98.9	98.7	98.7	99.0	98.4				
	7.5	7.8	4.1	7.6	6.1	7.6	6.3	6.0	6.2	5.6	5.9	7.0				
HR-ICP-MS (ppm)																
Y	57.9	16.2	54	15.1	49.6	38.1	17.2	15.7	15.4	4.64	15.2	23.2	30.3	29.1	16.5	36.6
La	52.6	11	32.7	5.76	25.1	15.4	7.94	6.68	10.2	2.68	8.81	11	16.9	16.3	0.641	23.7
Ce	145	37.6	75.3	27.9	38.1	33.9	31	31.7	28.1	19.4	28.1	33.1	36.1	38.9	1.96	51
Pr	14.5	3.69	9.88	1.97	5.75	5.19	2.62	2.49	3.29	1.09	2.99	3.73	5.36	5.13	0.357	6.48
Nd	56.7	15.4	42.7	8.81	25.6	23.6	12	11.9	14.7	5.21	13.8	16.9	24.2	23.5	2.27	27.2
Sm	11.8	3.76	9.97	2.36	6.13	6.39	3.06	3.41	3.59	1.42	3.49	4.35	6.04	5.78	1.07	6.18
Eu	2.31	0.837	2.67	0.776	1.84	1.56	0.593	1.33	1.17	0.546	1.35	1.14	1.99	1.9	0.472	1.85
Tb	1.79	0.652	1.61	0.415	1.12	1.13	0.508	0.582	0.548	0.209	0.555	0.7	0.958	0.918	0.34	1
Ho	2.05	0.824	1.83	0.497	1.39	1.33	0.553	0.603	0.565	0.204	0.56	0.762	0.981	0.924	0.529	1.19

Er	5.81	2.41	5.08	1.44	3.95	3.73	1.56	1.56	1.48	0.514	1.44	2.12	2.55	2.39	1.64	3.4
Tm	0.867	0.365	0.729	0.206	0.569	0.537	0.212	0.204	0.198	0.0635	0.189	0.291	0.341	0.321	0.245	0.494
Lu	0.763	0.337	0.65	0.189	0.519	0.466	0.169	0.152	0.154	0.0463	0.136	0.224	0.278	0.261	0.233	0.463
Li	0.478	0.298	9.34	16.2	41.3	45.7	47.2	33.4	52.8	25.1	33.9	25.4	4.85	4.6	2.97	9.22
Be	4.96	4.39	2.14	1.23	0.981	0.672	0.629	0.88	1.02	0.898	0.779	0.868	1.16	1.04	0.0941	2.59
Zr	365	313	282	266	216	246	272	218	208	214	218	255	180	173	14.9	180
Nb	72.4	70.6	35.1	25.9	19.7	20.4	27.7	19.5	19.2	22.5	20.6	23.8	19.1	18.6	0.561	12.7
Cs	0.291	0.323	0.456	0.0449	0.375	0.211	0.161	0.23	0.347	0.0893	0.275	0.0759	0.104	0.101	0.0038	1.1
Hf	10.5	8.84	7.81	6.24	4.97	5.42	6.62	5.34	5.01	5.33	5.27	5.96	4.33	4.07	0.561	4.57
Ta	4.76	4.53	2.14	1.59	1.16	1.21	1.63	1.22	1.13	1.32	1.22	1.42	1.14	1.07	0.0438	0.726
Pb	9.7	8.91	3.55	2.43	2.52	13.4	2.05	1.81	2.41	2.21	1.86	2.29	1.91	3.4	3.01	9.96
Th	7.52	2.9	2.81	1.52	1.34	1.14	1.2	0.917	0.911	0.365	0.82	1.11	1.13	1.05	0.0259	5.09
U	2.42	1.32	0.729	1.06	1.33	1.31	2.15	1.44	3.07	1.37	1.43	2.67	0.409	0.393	0.0184	1.55
Sc	4.61	1.65	37.7	10.8	39.5	36.9	27.7	36.8	25.6	8.16	26.3	22.3	36.4	34.6	42.4	35.9
Ti	2896	2680	18340	19240	15360	18690	22610	18920	18680	21310	20070	23250	16250	15470	5355	13360
V	15.5	14.3	415	497	342	469	586	489	399	538	431	536	330	306	306	418
Cr	10.7	17.9	137	76.8	80.4	192	84.9	119	151	131	128	135	383	348	356	20.4
Co	1.13	1.37	39.5	37.4	47.5	42.6	44.3	42.7	57.2	38	36.4	48.6	47.8	46.6	50	37
Ni	1.18	1.6	61.3	52.6	135	142	133	74.9	251	67	67.8	171	118	115	164	11.8
Cu	5.84	7.7	149	83.9	320	618	118	214	143	338	199	211	138	138	122	26.4
Ga	19.9	15.5	23.2	23.7	22.8	20.1	23.6	24.3	25.7	23.7	24.5	23.8	22.3	21.6	15.5	22.6
Ge	1.44	0.735	1.95	1.89	2.33	2.59	1.76	1.58	1.81	1.33	1.49	2.1	1.84	1.85	1.23	1.8
Rb	91.4	60.7	29.7	14.8	25.6	49.8	15.8	20.6	22.4	18.3	17.6	10.5	10.8	10.6	0.316	48
Sr	82	40.1	291	75.8	338	121	188	158	225	122	199	30	412	388	99.5	335
Ba	836	694	345	285	488	502	270	154	179	166	156	35.1	130	121	6.72	665
Eu	2.3	0.903	2.65	0.81	1.9	1.63	0.623	1.32	1.19	0.57	1.36	1.13	1.97	1.91	0.486	1.94
Gd	11.1	3.75	10.2	2.54	6.94	6.91	3.24	3.65	3.59	1.39	3.59	4.51	6.21	5.99	1.8	6.45
Dy	10.4	4.03	9.31	2.5	6.68	6.74	2.88	3.26	3	1.11	3.05	4	5.37	5.04	2.36	6.03
Yb	5.25	2.34	4.49	1.31	3.5	3.21	1.22	1.17	1.1	0.358	1.03	1.69	1.99	1.9	1.54	3.08
Tl	0.915	1.02	0.343	2.38	2.66	13.1	1.45	1.45	8.32	0.863	1.06	5.49	0.465	0.231	0.0302	0.924

Table S2. Zircon U-Pb data from DRA-C1 rhyolite, obtained by in situ Laser Ablation ICP-MS

						2 σ error		2 σ error			Age (Ma)	2 σ error
Analysis	Pb ppm[1]	Th ppm[1]	U ppm[1]	Th/U	$^{207}Pb/^{235}U$[2]	$^{207}Pb/^{235}U$	$^{206}Pb/^{238}U$[2]	$^{206}Pb/^{238}U$	Rho	$^{206}Pb/^{238}U$	$^{206}Pb/^{238}U$
Zr1/1	23	391	804	0.49	0.1915	0.0061	0.02713	0.00075	0.87	172.5	4.7
Zr1/2	37	978	1174	0.83	0.1935	0.0060	0.02776	0.00075	0.87	176.5	4.8
Zr1/3	32	768	1048	0.73	0.2041	0.0064	0.02741	0.00075	0.87	174.3	4.7
Zr1/4	42	886	1389	0.64	0.1965	0.0063	0.02744	0.00075	0.86	174.5	4.7
Zr1/5	34	724	1155	0.63	0.1984	0.0066	0.02738	0.00075	0.82	174.1	4.7
Zr2/1	5.3	185	154	1.20	0.1999	0.0113	0.02747	0.00081	0.52	174.7	5.0
Zr2/2	3.7	127	108	1.18	0.1937	0.0120	0.02732	0.00081	0.48	173.8	5.1
Zr3/1	2.1	59	50	1.19	0.4865	0.0383	0.02902	0.00108	0.47	184.4	6.7
Zr3/2	1.3	30	32	0.94	0.4527	0.0472	0.02952	0.00123	0.40	187.5	7.7
Zr5/1	5.3	125	159	0.79	0.2464	0.0196	0.02789	0.00093	0.42	177.3	5.8
Zr5/2	13	479	355	1.35	0.2662	0.0115	0.02724	0.00078	0.66	173.2	4.9
Zr7/1	1.8	41	60	0.69	0.1961	0.0144	0.02702	0.00081	0.41	171.9	5.1
Zr7/2	1.7	33	51	0.65	0.3266	0.0200	0.02812	0.00087	0.51	178.7	5.4
Zr7/3	2.1	53	67	0.80	0.1920	0.0143	0.02718	0.00081	0.40	172.9	5.2

[1]: concentration uncertainty c.20%

[2]: data not corrected for common-Pb

Figure S1. SiO_2 vs Loss of ignition (L.O.I.). A: intermediate samples (orange squares) and the basaltic sample DRA C2-1 (dark gray square). B: intermediate samples (orange squares), the basaltic sample DRA C2-1 (dark gray square) and the rhyolitic samples DRA C1-1 and DRA C1-2. Note the distinct correlation between SiO_2 and L.O.I. for samples of intermediate - compostions, which is characteristic of a SiO_2 leaching induced by seawater weathering.

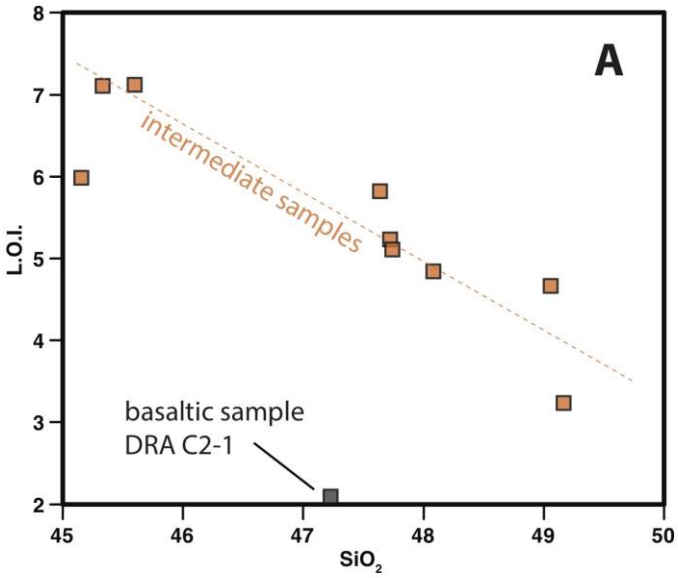

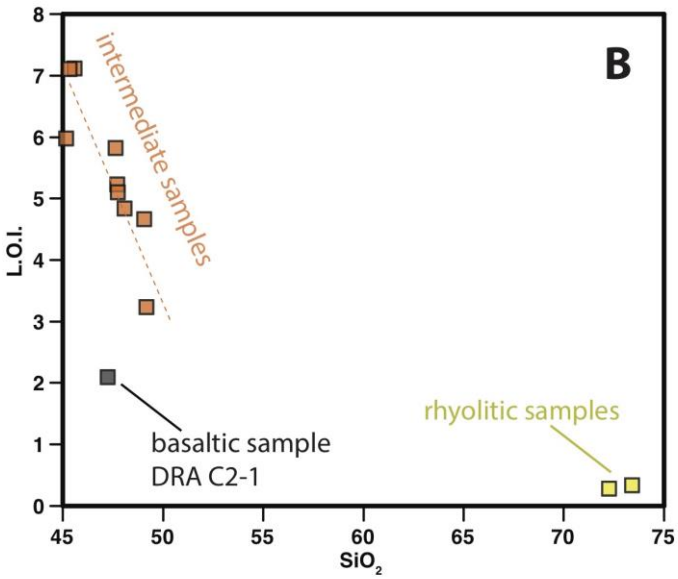

Figure S2. Ce/Ce* vs Nb/La in the basatic, intermediate and rhyolitic samples of this study. Ce* is estimated based on the averaged concentrations of La and Pr, normalized to the primitive mantle[58]. The apparent correlation between the rare earth element Ce and the high field strength element Nb, both non- fluid -mobile-elements under oxydative conditions (Ce_4^+) supports the possiblity of an apparent enrichment in these elements, due to the selective leaching of other rare earth elements. Nevertheless, the extent of the HFSE positive anomaly being approximately three times higher than Ce anomalies, it is likely that a pristine (i.e.: magmatic) enrichment in these elements was present before alteration.

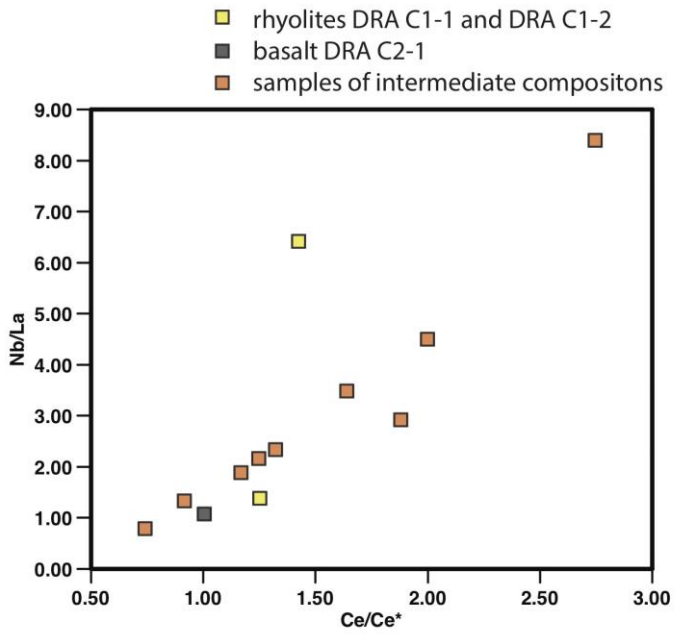

Figure S3. Position of the postulated Sierra Leone hotspot (red star) at 201 Ma, using the kinematic model of Müller et al[26]. The dashed contour indicates the position of the Blake Plateau by reference to North America. The Blake Plateau formed during the Lower Jurassic formation of the Central Atlantic[49]. Drawn from results using GPlates 2.0.0.

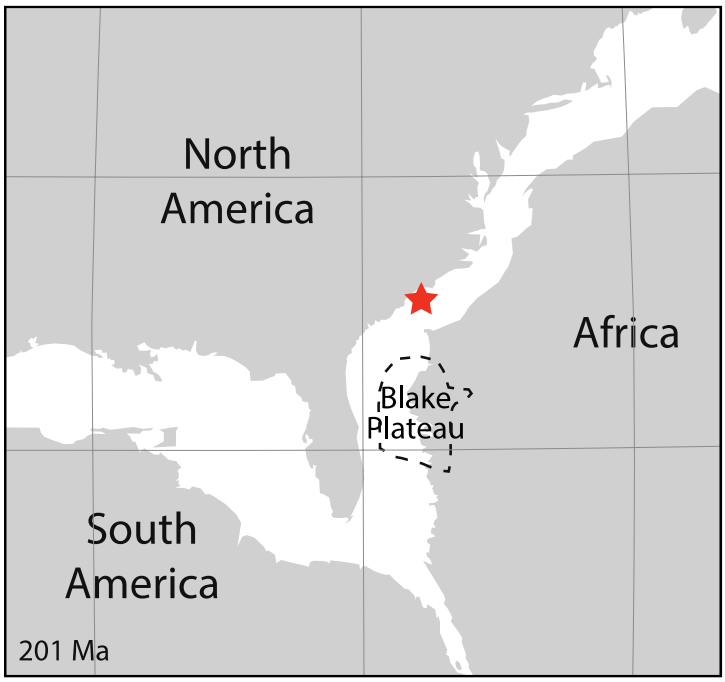

Figure S4. Measured international standards BHVO2, BIR1 and BCR2 compared to published referenced values[61, 62, 63]. Normalization values (primitive Mantle) are those of McDonough and Sun[58]. Measured and referenced values are similar within (2-10%).